JOURNAL OF MATERIALS SCIENCE 29 (1994) 736–741

Effect of antimony on the growth kinetics of aluminium–silicon eutectic alloys

S. KHAN
Metallurgy Division, A. Q. Khan Research Laboratories, G. P. O. Box 502, Rawalpindi, Pakistan

R. ELLIOTT
Material Science Centre, University of Manchester, Manchester M1 7HS, UK

On treating aluminium–silicon alloy with 0.2 wt% Sb, it was revealed that antimony refines the eutectic structure by reducing the interflake spacing rather than acting as a modifier. The growth mechanism is similar to the unmodified Al–Si flake structure, giving the relationships of the type $\Delta T = K_1 V^{0.51}$ and $\lambda = K_2 V^{-0.4}$, where K_1 and K_2 are constants. At high solidification rate, the transition from flake to fibre is observed. However, this transition occurs at lower velocity compared to quench modification of the pure alloy. The high magnitude of undercooling measured with the antimony-treated alloy is attributed to constitutional undercooling, which leads to extra refinement of the Al–Si eutectic structure.

1. Introduction

Liquid treatment of Al–Si eutectic alloys was introduced long ago by Pacz [1]. A drastic change in the structural properties was produced by adding sodium fluoride flux to the melt, which was termed a modification. Since then it has become the usual method for alteration of the Al–Si eutectic structure.

The most commonly used modifications at present are those using sodium/strontium. These modifications convert very efficiently the coarse eutectic into a fibrous eutectic structure. However, they have numerous drawbacks, such as their volatility and rapid rate of burn-out from the melt, their gassing tendency, reaction with and resulting damage to the crucible, and the inconsistent structure as a result of burn-out. When magnesium is present in Al–Si, the tendency for these drawbacks to occur is even higher.

Antimony-treated alloy is distinguished by low susceptibility to gassing, and due to excellent casting properties it produces very sound cast components. These alloys are at present used for numerous high-performance applications, including both heat-treatable and non-heat-treatable wheels and suspension arms for automobiles [2–5].

Antimony in Al–Si eutectic melt neutralizes phosphorus in a similar way to sodium/strontium. The antimony combines with magnesium to form a compound Mg_3Sb_2 which dissolves phosphorus. In the absence of magnesium, antimony combines with aluminium to form AlSb which has a similar effect to that of Mg_3Sb_2. The action of antimony is permanent in the Al–Si eutectic melt, and its refining action is completely unaffected by holding time, remelting, and degassing, which is not the case with sodium/strontium. The properties exhibited are similar to those of sodium/strontium-treated alloys. Tables I–III show the initial characteristics and improvement in the properties of Al–Si alloys when ternary additions are made [6, 7].

The subject of this work was to investigate the mechanism of structural refining of Al–Si eutectic in the presence of antimony.

2. Experimental procedure

The directional growth experiments were performed in order to measure the interface temperature (undercooling) and spacing as described in detail elsewhere [8, 9]. However, briefly the 99.99% pure aluminium and silicon of eutectic composition (12.6 wt % Si) were melted in a graphite crucible under an argon atmosphere. Addition of antimony was carried out by wrapping the antimony metal in a piece of aluminium foil and plunging it deep into the melt with a graphite rod. The melt temperature was maintained at 800 °C and it was stirred for a constant interval of time in order to dissolve the antimony metal completely in the melt. After homogenization, the molten alloy was sucked up into a pre-heated alumina tube by applying a vacuum. The specimen tube was then positioned in the Bridgman furnace for directional solidification. This was achieved by drawing the specimen from the furnace at a pre-determined rate directly into the water reservoir.

The directionally grown specimen was sectioned both longitudinally and transversely for examining the as-solidified structure. Chemical analysis of the grown specimen was carried out to measure the antimony build up at the interface on the polished specimens. The interface position was marked on the mount and coated with carbon. The microprobe analysis was done between 1.5 mm below and above the interface, so that the beam is traversed through the interface.

0022–2461

3. Results and discussion

Antimony treatment of liquid Al–Si eutectic alloys has been recognized as an alternative method of structural refinement to sodium/strontium. When antimony is added to Al–Si eutectic melt, the solidifying eutectic is refined by the reduction of interflake spacing. The structures appearing during the directional growth of pure and 0.2 wt % Sb-containing alloys are shown in Figs 1 and 2, respectively. The features show that a flake, rather than a fibrous, silicon structure is formed in the presence of antimony and therefore it behaves as a refiner of the interparticle spacing in the solidifying eutectic, instead of a modifier, Fig. 2c. The refining action is not as drastic as with sodium and strontium.

TABLE I [6] Comparison of founding properties of aluminium alloy

Alloy	Castability index	Hot tearing index	Volume change on freezing (%)
Al–7% Si–Mg	85	0.69	3.5
Al–4% Cu–Mg	64	3.89	8.7
Al–3% Mg–Mn	73	1.90	7.5

The transmission electron micrograph (Fig. 2a) shows the presence of twins in the antimony-refined flake. These twins are of the same nature as shown for pure Al–Si flake structure (Fig. 1a).

It has been reported that 0.1 wt % Sb is sufficient for the refining of the eutectic structure, after which the flake spacing increases as the concentration level of antimony is increased [7, 10]. However, it has been observed in the present study that the structural refining occurs at a concentration level of 0.2 wt % Sb.

The undercooling and interparticle spacing measured for antimony-treated alloy are given in Table IV and are plotted as a function of growth velocity in Fig. 3. These results reveal that the growth relationship can be described by the equations

$$\Delta T = 34\ V^{0.51}\ (^{\circ}\mathrm{C\,mm\,s}) \quad (1)$$

$$\lambda^{2.5} V = 3.24 \times 10^{-8}\ (\mathrm{mm\,s}) \quad (2)$$

These relationships display a similar form to that obtained for the flake structure [8, 9]. However, the interparticle (flake) spacing is slightly reduced and the undercooling is higher than measured for the flake structure in pure alloy. At high solidification rate, a

TABLE II Mechanical properties of directionally solidified Al–Si eutectic alloys (strontium and quench modified)

Structure	Growth velocity ($\mu m\,s^{-1}$)	Tensile properties		
		0.2% proof stress ($N\,mm^{-2}$)	UTS ($N\,mm^{-2}$)	Elongation (%)
Flake	45	53.8	142	8.5
Flake–fibre	450	60.6	155	12.5
Flake–fibre	1300	63.6	157	8.8
Chill cast	–	101.5	220	3.8

TABLE III Mechanical properties of antimony-treated Al–Si alloys

Growth velocity ($\mu m\,s^{-1}$)	Sb content (wt %)	Tensile strength ($kg\,mm^{-2}$)	0.2% offset yield ($kg\,mm^{-2}$)	Hardness, H_v	Elongation (%)
20	0	12.64	5.57	55.15	3.5
50	0	13.52	6.72	58.23	3.8
500	0	15.47	7.36	68.08	3.7
20	0.2	14.46	8.09	61.26	5.0
50	0.2	16.04	8.30	63.56	7.8
500	0.2	18.24	8.93	74.39	7.3

TABLE IV Directionally solidified Al–12.6 wt % Si–0.2 wt % Sb alloy, $G = 122\,^{\circ}\mathrm{C\,cm^{-1}}$

Growth velocity ($cm\,s^{-1}$)	Lead distance (cm)	Growth temp. (°C)	Undercooling $\Delta T = T_E - T_G$ (°C)		Interparticle spacing (cm)	
10.8	0.31	573.8	3.4		5.4	
28.8	0.3	572.5	4.7		4.7	
54.0	0.22	570.0	7.2		2.9	
108.0	0.205	566.8	10.4		2.5	
205.0	0.095	563.4	13.8		2.0	
308.0	0.15	562.0	15.2		1.7	1.57[b]
505.0	0.131	567.5	–	9.7[a]	–	1.30[b]
807.0	0.13	563.3	–	13.9[a]	–	1.17[b]
875.0	0.06	562.1	–	14.6[a]	–	–

[a] Undercooling measured for quench modified samples in the presence of antimony.
[b] Spacings measured for quench modified samples in the presence of antimony.

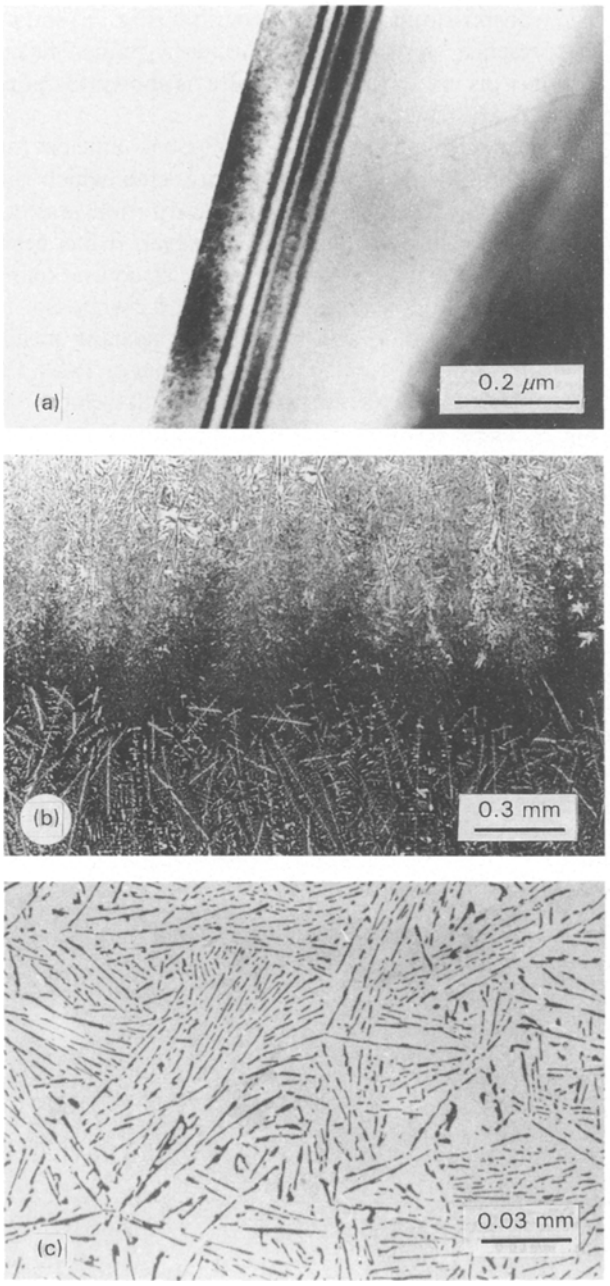

Figure 1 The structural features of unmodified Al–Si eutectic, solidified at 104 $\mu m\,s^{-1}$. (a) Co-zonal twinning in the silicon flake. (b) Longitudinal section showing the quench interface. (c) Transverse section of the above sample.

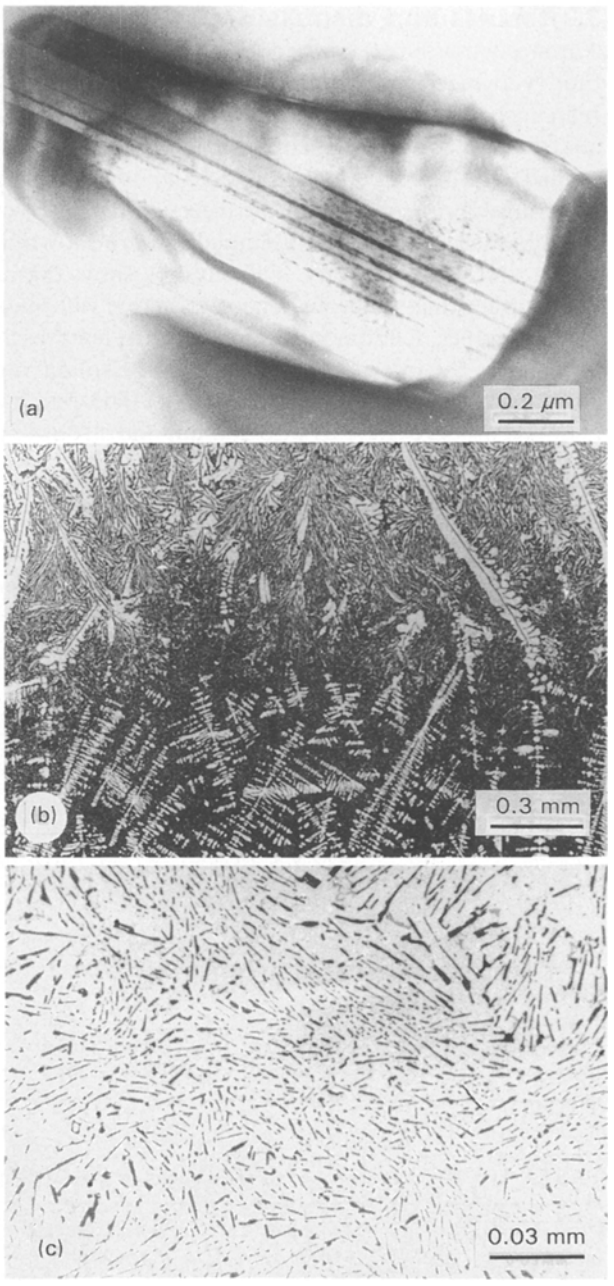

Figure 2 The structural features of Al–Si eutectic in the presence of antimony, solidified at 104 $\mu m\,s^{-1}$. (a) Twinning in a silicon flake in the presence of antimony. (b) Longitudinal section showing the quench interface. (c) Transverse section of the above sample.

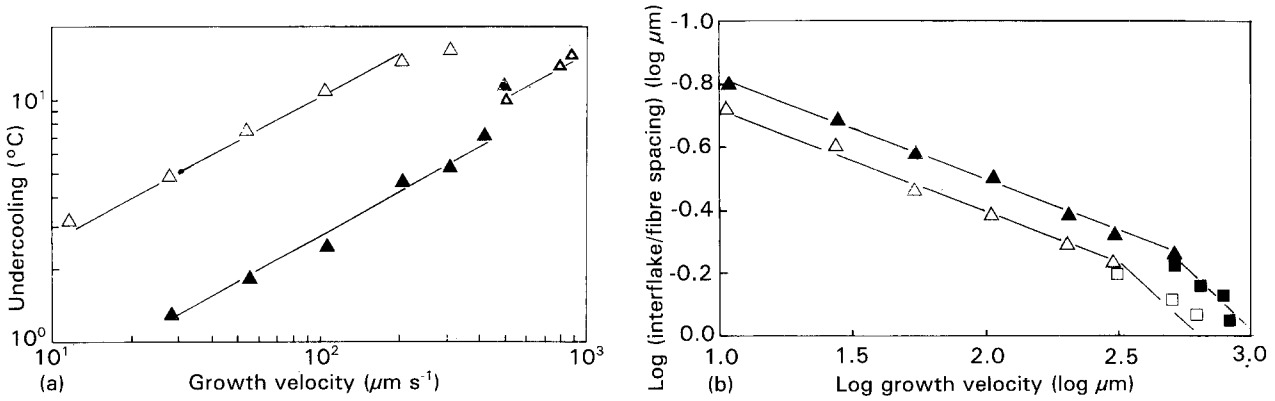

Figure 3 (a) Undercooling for (▲) pure and (Δ) 0.2 wt % Sb-treated alloys plotted as a function of growth velocity. (Δ) Drop in undercooling in the presence of antimony. (b) The variation in spacings of (▲) pure and (Δ) 0.2 wt % Sb-treated Al–Si eutectic alloys. (■) chill fibres, (□) chill fibres with antimony.

similar type of transition occurs, as in the quench modification. However, this transition is at lower velocity as compared to quench modification [9–11]. This is perhaps due to the dual refining action of silicon flake structure which tends to undergo a change in the structure at lower velocity. After transition the value of undercooling obtained for fibrous structure is not as low as chill modification, and spacing values are slightly reduced. The structural features developed at growth velocities of 308 and 807 $\mu m\,s^{-1}$ are shown in Fig. 4a and b respectively. The structural features obtained at high solidification rate (807 $\mu m\,s^{-1}$) are similar to that of the quench-modified structure [9, 11, 12]. Microprobe analysis in Fig. 5 shows the antimony build up ahead of the interface. All these observations suggest that different phenomena have occurred during the eutectic solidification of the antimony-treated alloys.

Kisak-u-rek [7] has proposed that there is a possibility of antimony adsorption on the interface and poisoning of the re-entrant twin grooves, leading to more frequent twinning with a large growth undercooling. This action is similar to that accepted for the influence of sodium and strontium. However, in a recent model proposed by Shu-Zu-Lu and Hellawell [13] which related to the atomic radii of the modifier, it is shown that the size factor requirement, i.e. atomic radius of a modifier/atomic radius of silicon (R_i/R_{Si}), should be greater than 1.654, which is the primary factor for impurity modification. Table V gives the atomic radius ratio of strontium, sodium and antimony, from which it is clear that antimony does not fall in this size ratio.

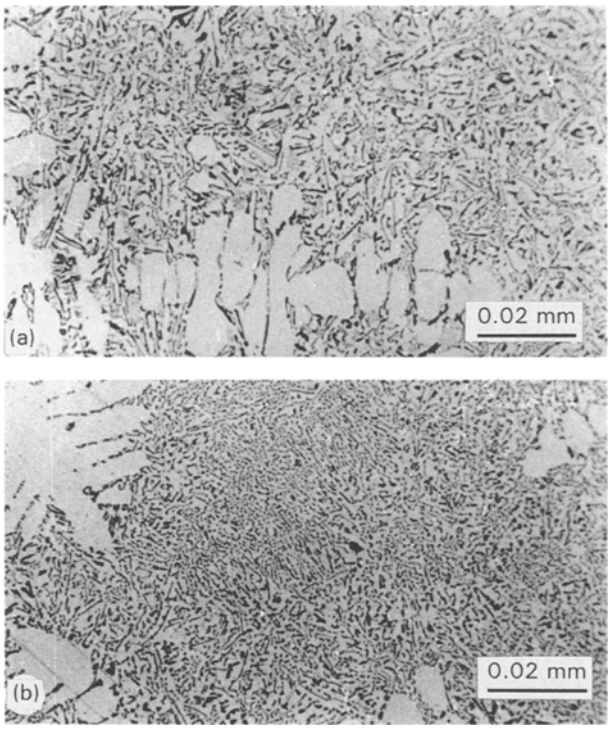

Figure 4 Structural features obtained at high solidification rate in the presence of antimony. (a) A mixed form of flake and fibrous structure which appeared at 308 $\mu m\,s^{-1}$. (b) Completely fibrous structure formed at 807 $\mu m\,s^{-1}$.

If antimony does not poison the re-entrant grooves, it is most likely to build up at the interface during solidification, which is evident in Fig. 5. This may lead to the constitutional undercooling.

However, simple analysis can be carried out in order to understand the phenomenon of eutectic solidification in the presence of antimony. The liquidus temperature distribution ahead of the interface is given by [6].

$$T_e = T_o - mC_o[1 + (1 - K_o)/K_o \exp(-VX/D)] \quad (3)$$

where T_o is the melting point of the solvent, m is the liquidus slope, C_o is the solute content, K_o is the equilibrium distribution coefficient, V is the growth velocity, D is the diffusion coefficient and X is the distance into the liquid from the solid–liquid interface. This equation gives the amount of constitutional undercooling ahead of the interface, knowing the temperature gradient in the liquid ($G = 122\,^{\circ}C\,cm^{-1}$). For this purpose the value must be chosen for m, K_o and D. The antimony profile shown in Fig. 5 leads to a value of $K_o = 0.15$. A value of $2 \times 10^{-5}\,cm^2\,s^{-1}$ was chosen for D. However, the selection of a value for m is more difficult in the absence of detailed information about the phase diagram for the Al–Si–Sb system. A value of $m = 8\,^{\circ}C\ (wt\,\%)^{-1}$ was arbitrarily chosen in the present conditions. It must be pointed out that the value selected for m does influence the magnitude of the

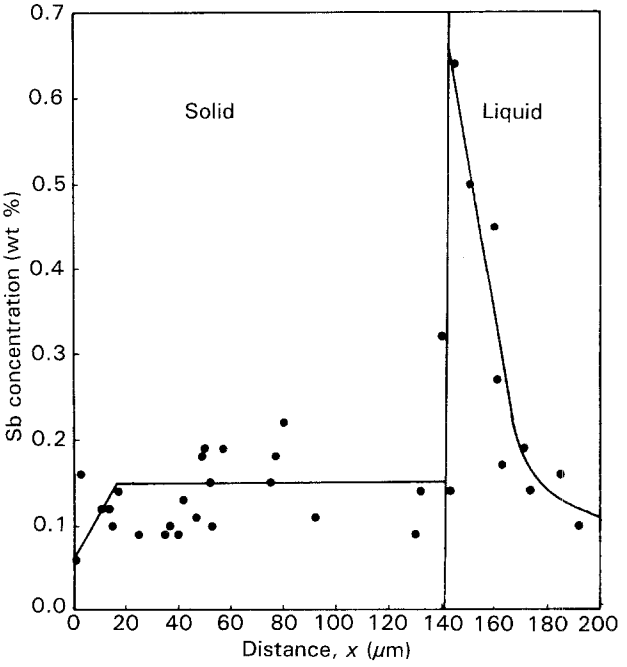

Figure 5 Microprobe analysis for antimony solute build-up at the interface obtained at 104 $\mu m\,s^{-1}$.

TABLE V R_i = atomic radius of modifier, R_{Si} = atomic radius of silicon

Element	R_i (nm)	R_{Si} (nm)	R_i/R_{Si}
Na	0.185	0.117	1.58
Sr	0.216	0.117	1.84
Sb	0.16	0.117	1.36

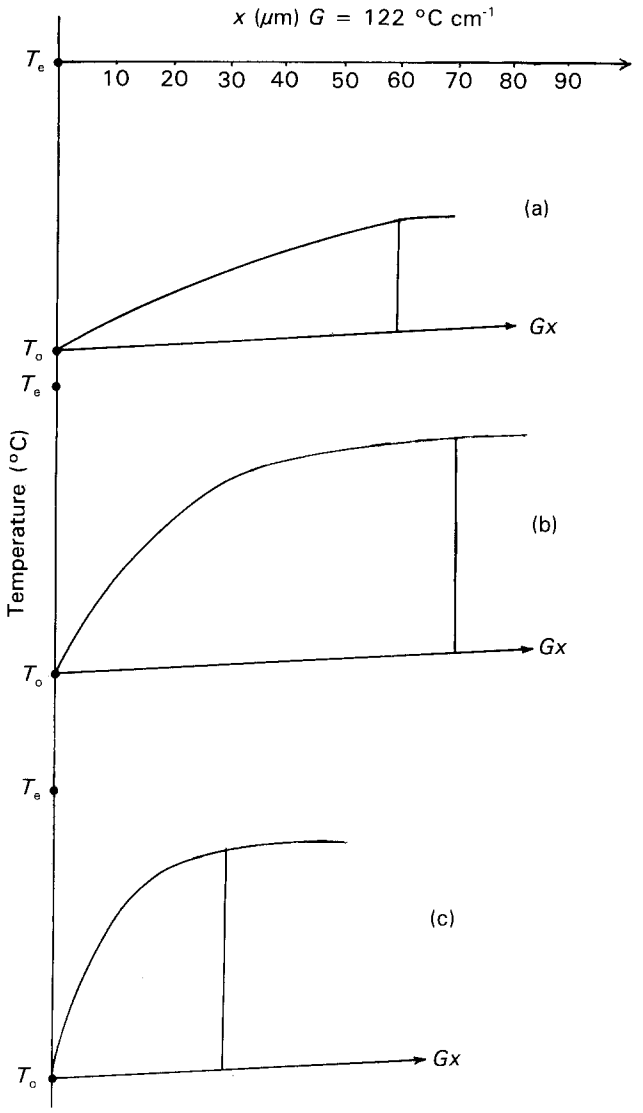

Figure 6 Calculation of constitutional undercoolings. (a) $V = 28\ \mu m\,s^{-1}$, $\Delta T = 3.1\,^{\circ}C$; (b) $V = 104\ \mu m\,s^{-1}$, $\Delta T = 7\,^{\circ}C$; (c) $V = 205\ \mu m\,s^{-1}$, $\Delta T = 7.7\,^{\circ}C$.

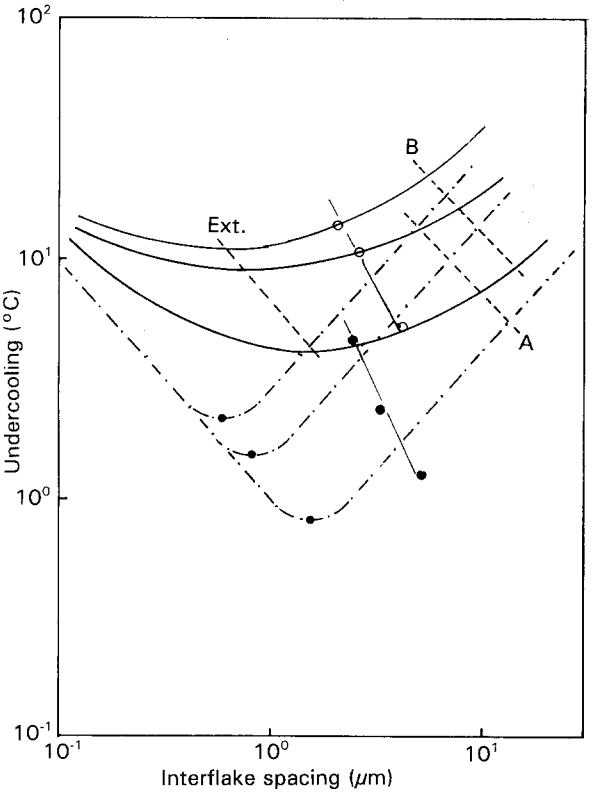

Figure 7 (——) The change in the shape of the growth curve for flake structure in the presence of antimony with the additional term $\Delta T_{C.U}$. (●) The operative growth points for pure Al–Si flake structure, and (○) for the antimony-treated Al–Si alloys.

constitutional undercooling and, consequently, it is unfortunate that detailed phase-diagram information is not available. Fig. 6 explains the features of these calculations at $G = 122\,^{\circ}C\,cm^{-1}$. This leads to undercooling value of 3.1, 7 and 7.7 °C for growth velocities of 28, 104, 205 $\mu m\,s^{-1}$, respectively. It is assumed that the interface undercooling in the presence of antimony is given by

$$\Delta T = \Delta T_D + \Delta T_C + \Delta T_{C.U} \quad (4)$$

Hence

$$\Delta T = K_1 V\lambda + K_2/\lambda + \Delta T_{C.U} \quad (5)$$

It is possible to construct growth curves using Equation 5 for the above-mentioned growth velocities. These velocities are chosen to ensure that within this range the morphology is completely flake. In Fig. 7 the change in the shape of the growth curves by adding the term $\Delta T_{C.U}$ in Equation 5 is shown. The Magnin and Kurz [14] theory, recently proposed for the flake structure, claims that this model behaves significantly with respect to Fe–C flake structure. However, the detailed analysis of the Magnin and Kurz theory is shown elsewhere [8, 9] with respect to the experimental data of unmodified Al–Si alloy. It will be convenient to explain the growth behaviour of Al–Si eutectic in the presence of antimony, if the Magnin and Kurz theory is introduced into the new growth curves by incorporation of $\Delta T_{C.U}$, such that

$$\Delta T = K_1 V\lambda + K_2/\lambda + F + \Delta T_{C.U} \quad (6)$$

Dotted line B shows the displacement of the Magnin and Kurz theory due to the additional term $\Delta T_{C.U}$; although there is a considerable displacement of the theoretical line, however, it is still parallel to the line joining the extremum points, as predicted by the theory. If the experimentally measured operative points for Al–Si–Sb eutectic for $G = 122\,^{\circ}C\,cm^{-1}$ are inserted into the new growth curves, they lie exactly on the curves and show a similar deviation from the theory as observed for the unmodified flake growth.

The same procedure can be adopted for fibrous structure in the presence of antimony. The growth curves are plotted using a constant due to Hogan and Song [15], $K_1 = 2.17 \times 10^{-3}\,^{\circ}C\,s\,\mu m^{-2}$ and $K_2 = 0.214\,^{\circ}C\ \mu m$, for velocities of 505 and 807 $\mu m\,s^{-1}$. The calculated values of constitutional undercooling for these velocities are 8.1 and 8.2 °C respectively. Fig. 8 shows the change in the shape of the growth curves for fibrous structure by adding the term $\Delta T_{C.U}$. The operative growth points show a similar behaviour in the two chill-modified cases. However, the undercooling is much greater in the antimony-containing alloy and this is attributed to constitutional undercooling.

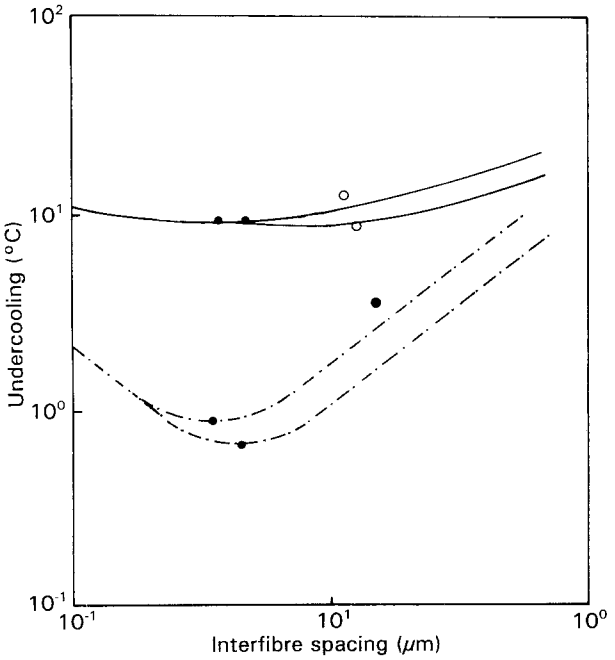

Figure 8 (——) The change in the shape of the growth curve for fibrous structure in the presence of antimony with the additional term $\Delta T_{c,u}$. (●) The operative growth point for pure quench-modified fibre, and (○) for the antimony-treated chill-modified fibres.

This simple analysis has been carried out in order to provide evidence that in the presence of antimony, the growth behaviour is similar to that of the flake or to that of the fibrous structure in the case of quench modification. However, the eutectic structure is slightly refined in the two cases at the expense of constitutional undercooling. It gives support to the hypothesis that antimony refines the structure due to constitutional undercooling and does not modify it.

3. Conclusion

Antimony behaves as a refiner rather than a modifier in the solidifying eutectic. The growth mechanism is similar to the unmodified flake in the presence of antimony. The growth relationships found in the presence of antimony are of a similar type to that obtained for the flake structure in pure alloy. The additional undercooling measured is attributed to constitutional undercooling for refining of the flake structure. The introduction of Magnin and Kurz's theory to explain the growth behaviour of antimony-treated alloy shows the similar deviation as found for flake structure. At high growth velocity, the growth kinetics are similar to quench modification.

Acknowledgements

This work was performed at the Material Science Centre, University of Manchester. The authors thank Professor F. R. Sale for provision of laboratory facilities and the Ministry of Science and Technology, Government of Pakistan, for funding this project. The authors also thank Dr F. H. Hashmi and Dr A. Q. Khan for support and useful comments, and Dr Anwar-ul-Huq for reviewing this paper.

References

1. A. PACZ, US Pat. 1387900 August 1921.
2. G. NAGEL and R. PORTALIER, *Int. Cast Metals J. AFS* **5** (4) (1980) 2.
3. R. SHARAN and N. P. SAKSENA, *ibid.* **3** (1) (1978) 29.
4. J. CHARBONNIER, J. J. PERRIER and R. PORTALIER, *ibid.* **3** (4) (1978) 17.
5. P. DANAMI and M. GHAFELEHBASHI, *Br. Foundry Man Soc.*, **72** (1) (1979) 4.
6. R. ELLIOTT, "Eutectic Solidification Processing", Butterworth Monograph in Materials (Butterworth's, London, 1983).
7. S. E. KISAK-U-REK, paper presented at the World Foundry Congress, 7–12 September, Prague, Czechoslovakia (1986).
8. S. KHAN and R. ELLIOTT, *Acta Metall.* **41** (1993) 2433.
9. S. KHAN, PhD thesis, University of Manchester (1990).
10. S. B. YANEVA, N. V. STOICHEV and A. D. PANAJETAVA, *Cryst. Res. Technol.* **16** (1991) 737.
11. S. KHAN, in Conference Proceedings, "2nd International Symposium on Advance Material", 15–19 September, Islamabad, Pakistan (1991).
12. S. KHAN, paper presented at the 4th National Symposium on Frontiers in Physics, Quiad-i-Azam University, 15–19 April, Islamabad, Pakistan (1992).
13. SHU-ZU-LU and A. HELLAWELL, *Metall. Trans.* **18A** (1987) 1721.
14. P. MAGNIN and W. KURZ, *Acta Metall.* **35** (1987) 1119.
15. L. M. HOGAN and H. SONG, *Metall. Trans.* **9A** (1987) 1036.

Received 9 November 1992
and accepted 19 March 1993